Structure development in aggregates of poorly developed soils through the analysis of the pore system

UNIVERSITÀ DEGLI STUDI DI TORINO

Structure development in aggregates of poorly developed soils through the analysis of the pore system

Gloria Falsone, Eleonora Bonifacio and Ermanno Zanini

Università degli Studi di Torino, DIVAPRA, Chimica Agraria e Pedologia

Corresponding Author G. Falsone, *Present address*

Università degli Studi di Bologna, DISTA
Via Fanin, 40 – Bologna, 40127 Italy
Tel: +39 051 209 6229; Fax: +39 051 209 6203
Email: gloria.falsone@unibo.it

Abstract

Aggregate porosity is the result of structural development, in turn controlled by pedogenic processes, which allow a soil to acquire specific characteristics and to lose those more related to the parent material. Porosity in sediments can be evaluated through simple packing models that provide an ideal porosity (Φ_{ideal}), which is based on soil particle size distribution only. As such they are not suitable for complex systems such as soil and aggregates. We evaluated therefore if the disagreement between ideal porosity and experimental data (ΦHg_T) is related to chemical properties and to the presence of specific diagnostic horizons, hence to soil development. The porosity underestimate, evaluated as $\Phi Hg_T/\Phi_{ideal}$ ratio, was the highest (up to 5-times) in Inceptisols and in their cambic horizons or in mollic epipedons. Thus, where pedogenesis is expressed enough to influence soil properties to such an extend to define diagnostic horizons, the ideal porosity model failed the most in describing the complexity of the void arrangement in the aggregates. Organic matter (OM) is a key factor in determining structural complexity, not only through its accumulation in surface horizons, as evidenced by the correlation between $\Phi Hg_T/\Phi_{ideal}$ and organic carbon (r=0.58), but also in deeper horizons. At the soil surface, independently from soil orders, OM contributed to structure development also through the poorly decomposed fractions. However, as also suggested by the weak linear dependence of the organic carbon-to-total nitrogen ratio on the porosity underestimate (r^2=0.51), it was evident that neither the quantitative, nor the qualitative data could fully explain the effects OM had on structure. Some specific spatial arrangement of particles, such as the typical hierarchical aggregation of mollic epipedons, must be taken into account to better understand the OM effects. In the subsoils, where the weathering process has led to a more complex structure, the effect of OM is enhanced by the concomitant presence of charged mineral surfaces.
In Inceptisols, calcium is a co-dominant factor in structural development (r=0.84), as expected when the formation of clay polyvalent cation-organic matter complexes occurs. In the least developed soils, pedogenic processes had a minimal effect on soil properties, and the aggregate porous system still retains some of the characteristics of the parent material, leading to a less pronounced underestimate by the ideal porosity model.

1. Introduction

Soil structure refers to the distribution and arrangement of soil voids and particles (Bronick and Lal, 2005). In the last years, it has received much attention because of its importance in affecting the role of soils as carbon sinks. On the other hand, soil organic matter (OM) is one of the main responsible of soil structure and aggregate dynamics (Six et al., 2004). Thus, carbon accumulation and structure development are two closely related soil forming process (Blanco-Canqui and Lal, 2004) active since the very initial steps of soil evolution. Particularly in slightly to moderately developed soils, such as Entisols, Inceptisols and Mollisols, additional processes can affect soil structure development, and the understanding of structure changes related to the on-going of soil evolution could provide some new insights into the complexity of the relation between OM and aggregates dynamics.

When considering the highest level of the USDA soil classification, Entisols are the weakest developed soils and they are the evolution precursors of all other soil orders (Nordt et al., 2000). In Entisols several pedogenic processes can occur and promote structural development, but none is expressed enough to deeply influence soil properties (Bockheim and Gennadyiev, 2000) that are therefore largely inherited from the parent material. Inherited primary particles have specific physical properties and packing characteristics, however their importance as primary soil constituents is reduced when organic matter, amorphous materials and cementing agents are abundant (Skopp, 2000). When structural development is driven by the accumulation of organic C in the upper soil profile and no severe leaching occurs, a well-structured mollic epipedon may develop. The mollic epidedon is mainly defined in term of its morphological characteristics (Soil Survey Staff, 1999), such as thickness, colour and structure. The presence of this diagnostic horizon allows to recognise the order of Mollisols, that, generally, have not undergone intensive weathering. In contrast, the development of soil structure caused by the on-going of weathering differentiates Entisols from Inceptisols. These

latter typically have a weakly developed subsoil horizon (i.e. the cambic horizon) resulting from physical alterations and chemical transformations to such an extent as to destroy the original rock structure or to form soil structure (Soil Survey Staff, 1999); a fundamental role of inorganic binding agents is thus expected.

Soil structure properties related to field macromorphological scale are essential in soil classification, and are caused by external factors, such as bioturbation or other disturbances, superimposed on the intrinsic properties of the solid phase. In particular, the same binding agents that originate the field scale structure of soil horizons are active also at a much lower scale being the components of the basic aggregate units Cl-P-OM (Edwards and Bremner, 1967; Tisdall and Oades, 1982; Oades and Waters, 1991). Organic molecules (OM) are associated to clay (Cl) through polyvalent cations (P) and the Cl-P-OM units join then together to form larger aggregates. The consequent relationships among sizes will affect soil physical properties that are, therefore, not only caused by the characteristics of large visible clods and are maintained also in disturbed samples, being soil aggregate the elementary units building bulk soil structure.

Although soil structure cannot be measured directly, it is commonly inferred by measuring the properties of the two components of aggregates (i.e., voids and particles) in defined size ranges. For very simple systems, such as sediment mixtures of finer and coarser particles, Clarke (1979) stated that the total volume of voids, i.e. porosity, was related to particle diameters, volume of solid fractions and packing arrangements of the components. In his proposed ideal packing model, the porosity is the result of void infilling and the porosity minimum of the mixture theoretically occurs when small particles completely fill the voids among larger particles. Koltermann and Gorelick (1995) stated that the ideal packing model underpredicts the porosity even in simple sediment mixtures, because it is based on the assumption that only one type of packing arrangement occurs. To measure the porosity in

natural complex systems, such as soil aggregates, one of the most frequently used method is mercury intrusion porosimetry (Lowell and Shields, 1999; Vidal Vázquez et al., 2008). The analysis of the cumulative curve of intruded mercury volume proposed by Bruand and Prost (1987) allows moreover to relate the aggregate pore volume to a modal equivalent pore size resulting from the interaction of the coarse grains with the clay phase, or from the packing of clay particles within the clay phase (Fiès and Bruand, 1998), and thus provides information about the specific particle arrangement of each size class in soil aggregates (Falsone and Bonifacio, 2009). Particle arrangement in soil aggregates does not only depend on particle size, volume and packing type, but is the result of structural development, which involves complex variations in the shape and type of the aggregate components. Thus, the disagreement between ideal predicted and measured soil porosity should be enhanced with respect to sediments and related to the different levels of complexity of aggregate structure. The aim of this study is therefore to evaluate if any disagreement between ideal predicted porosity and experimental data can be ascribed to soil development in slightly to moderate developed soils (Entisols, Inceptisols and Mollisols), and if the disagreement can be used as a quantitative descriptor of the degree of aggregate development in relation to specific pedogenic processes. We discuss moreover the changes occurring in the OM-porosity relationships.

2. Materials and Methods

Study area and sampling

The study area is located in the basin of the Camastra River in the mountain zone of the Basilicata region, in southern Italy (40°22'-40°35' N, 15°42'-16°01'E). The area is ascribed to the Italian soil region of "Apennine and anti-Apennine relieves on sedimentary rocks of

central and southern Italy" defined by Costantini et al. (2004). The study area is characterised by an elevation ranging from 450 to 1200 m asl, and the annual rainfall varies from 700 to 1000 mm, depending on elevation. Pastures start at about 1000 m asl, while oak and mixed forests prevail at lowest elevation. Geology is highly variable; carbonates and dolomites are typical of mountain massifs, and marls prevail on ancient river terraces. Lower positions in the relief are sometimes covered by more recent sand and silt deposits and conglomerate formations. Argillites and carbonatic sandstones are also present in the highlands. A full description of the study area can be found elsewhere (Zanini et al., 1995). After a preliminary soil survey, representative soil profiles were selected where site conditions allowed the development of Entisols, Inceptisols or Mollisols (Table 1).

The final dataset comprises twenty-nine soil samples collected from genetic horizons of some Entisols, Inceptisols and Mollisols , which were therefore characterised by the presence or absence of ochric or mollic epipedons and cambic subsurface horizons. The moisture regime of all profiles was ustic as estimated with the Newhall Simulation Model (Newhall, 1972) revised by Van Wambeke (2000). All soils are homogeneous at the great-group level: they are Ustorthents, Eutrusteps and Haplustolls, showing therefore no additional specific diagnostic features.

Analytical methods

The samples were air-dried and sieved to 2 mm. On the fine earth fraction, the pH was determined potentiometrically using a 1:2.5 soil:deionised water ratio. The Walkley-Black wet-oxidation method was used to determine the organic C content (Nelson and Sommers, 1982), while total N was determined by the Kjeldhal method (Bremner and Mulvaney, 1982). The CEC was determined using the $BaCl_2$-method (Rhoades, 1982) and the exchangeable Ca was measured in the extracts by atomic absorption spectroscopy (Perkin Elmer 3030). The

amount of iron oxides (Fe_{DCB}) was estimated after extraction with a Na-dithionite-citrate-bicarbonate solution (Mehra and Jackson, 1960). The particle size distribution was obtained by the pipette method (Gee and Bauder, 1986). On the 1-2 mm aggregate class, obtained by dry sieving, the cumulative pore volume curve was determined using a Hg porosimeter (Porosimeter 2000 WS equipped with a Macropore unit 120, CE Instruments) by step measuring the pressure required to force Hg into the pores and the volume of intruded Hg at each step. Mercury intrusion was performed up to 200 MPa of applied pressure. Assuming that the pores are cylindrical, the relation between equivalent pore radius (R expressed in µm) and applied pressure (P expressed in MPa) is described by the equation (Washburn, 1921):

$$2R = \frac{-4T\cos\alpha}{P} \quad (1)$$

where T is the surface tension of mercury and α its contact angle with the soil material. The values of T and α were taken as 0.480 N m^{-1} and 141.3°, respectively. For irregularly shaped pores, the ratio between the pore cross-section (related to the pressure exerted) and the pore circumference (related to the surface tension) is not proportional to the radius and depends on the pore shape. The equivalent pore size calculated by the equation (1) will thus be lower than the exact pore radius. However, although soil pores are rarely cylindrical in shape, the Washburn's equation is normally used to calculate the equivalent pore size from mercury porosimetry data (Lowell and Shields, 1991). At the highest level of applied pressure, the smallest measurable radius was 0.0037 µm.

Physical data treatments

The total volume of intruded Hg (i.e. total pore volume) was expressed on a mass basis (mm^3 g^{-1}, V_{HgTot}) and the total porosity (Φ_{HgT}, dimensionless) was routinely calculated from the data. The cumulative curve of intruded Hg volume as a function of the pore radius was used

to calculate the variation of the pore volume as a function of the log-transformed radius, finding the slope between the pore radii *Ri* and *Rj* (Bruand and Prost, 1987):

$$slope_{ij} = \frac{V_i - V_j}{\log_{10} R_j - \log_{10} R_i} \quad (2)$$

where the volumes V_i and V_j correspond to the radii R_i and R_j at two successive positions *i* and *j*. The values of the slopes were then plotted against the mean log radius. The relative maxima of the slope curve indicated the most represented classes of pores. Each peak thus corresponded to a radius that was taken directly from the graph. This radius was termed modal radius (expressed in µm). The volume of each modal class of pores was thus included between two minimum values of the slope, which defined the limits of the class. This data treatment typically allows to evince a bimodal or trimodal distribution. In case of bimodal distribution, the presence of a pore class with diameter < 0.05 µm whatever the clay content allows to identify the pores originated by the arrangement of fine particles (clay), whereas the large pore class is ascribed to that of coarser particles, i.e. sand and silt (Fiès and Bruand, 1998). We thus labelled the modal pore radii as *Rf* and *Rc* and attributed them to the packing of finer and coarser particles, respectively; the corresponding volumes of pores were labelled as V_{Hgf} and V_{Hgc}, i.e. volume of pores within the finer and coarser particles. The volume of solid particles of each fraction (*Vsf* and *Vsc*, volume of finer and coarser solids, respectively) was calculated using the data from textural analyses for particle mass and the particle density (ρ_s, g cm^{-3}) calculated using the regression equation based on the percentage total organic C, where ρ_s=2.583-0.025 total organic C (Rühlmann et al., 2006). The total volume of finer and coarser particles (*Vf* and *Vc*, respectively) was the sum of voids and solids.

The measured total porosity (Φ_{HgT}) was compared to the predicted ideal porosity (Φ_{ideal}) estimated according to the ideal packing model (Clarke, 1979). The quantitative relations developed for the ideal packing model are described in the works by Koltermann and Gorelick (1995) and Kamann et al. (2007). Briefly, for a mixture of coarse and fine particles,

the ideal porosity derives from an arrangement in which fine particles fill the voids among the coarser particles (coarse packing) or coarse particles are suspended in the matrix of fine particles (fine packing). This latter case originates when the volume of the finer component is greater that the porosity of the coarser fraction. In the coarse packing, the volume of the mixture is equal to the volume of the coarser component minus the volume of the finer particles (solids). In the ideal fine packing, the porosity is solely a function of the volume fraction and of the porosity of fine particles.

In ideal coarse packing, according to Kamann et al. (2007), when the volume of the premixed finer component (VF) is less than the volume of the voids within the coarser particles (VVC), the total volume of the mixture (VM) is assumed to equal the total volume of the premixed coarser component (i.e., volume of solids and voids of the coarser component, VC). The mixture porosity (Φ) is determined by how much VVC is reduced by the volume of solids of finer particles (VSF), and it is calculated as:

$$\phi = \frac{VVM}{VM} = \frac{VVC - VSF}{VC}; \quad VF < VVC \tag{3}$$

where VVM is the void volume of the mixture. When VF increases and equates VVC, the finer components fill all pores within the coarser fraction. The mixture porosity reduces towards a minimum (Φ_{min}) and is equal to the product of the porosities of each component:

$$\phi_{\min} = \frac{VVC}{VC}\frac{VVF}{VF}; \quad VF = VVC \tag{4}$$

where VVF and VVC are the volume of voids within the finer and coarser particles, VC and VF are again the total volume (i.e., volume of voids and solids) of the coarser and finer particles.

In ideal fine packing, the volume of pore space that would exist in the coarser fraction alone is lost and coarser particles are dispersed in the matrix of the finer component. The mixture total

volume (VM) is given by the sum of VSC (volume of the coarser solids) and VF. The pore spaces of the mixture exist only within the finer component and the porosity is:

$$\phi = \frac{VVF}{VM} = \frac{VVF}{VF + VSC}; \quad VF > VVC \tag{5}$$

For each sample we evaluated the total ideal porosity (Φ_{ideal}) using the volume of voids and solids obtained by Hg porosimetry after treatment of the data according to Fiès and Bruand, (1998). The total volume of coarser component was *Vs*, and V_{Hgc} and *Vsc* were the volumes of the voids and solids, respectively, within it. The total volume of finer component was *Vf*, and V_{Hgf} and *Vsf* were the volumes of the voids and solids within it. In our samples we always had $Vf \neq V_{Hgc}$, thus Equations 3 and 5 were rearranged as follows:

$$\phi_{ideal} = \frac{V_{Hgc} - Vsf}{V_{Hgc} + Vsf + Vsc}; \quad Vf < V_{Hgc} \tag{6}$$

$$\phi_{ideal} = \frac{V_{Hgf}}{V_{Hgf} + Vsf + Vsc}; \quad Vf > V_{Hgc} \tag{7}$$

Statistical data treatment was carried out using the package PASW v.18.0. The correlations between variables were calculated using Pearson's coefficient, after a visual inspection of the data to verify that the relationship was linear. The one-way analysis of variance, using soil orders or horizons as independent variables, was carried out after checking the homogeneity of variance by the Levene test. Differences among groups were estimated with a post-hoc Duncan test. A probability level of 0.05 was always used as threshold for significance.

3. Results

All soil samples had a neutral to basic reaction (Table 2). The organic carbon (OC) contents strongly varied among horizons: on the average the maximum was found at the surface of Inceptisols (47.5 g kg^{-1}) whereas the minimum (3.9 g kg^{-1}) was in the C horizons from Entisols. The OC/N ratio ranged from 12.5 to 5.2. A high variability was observed also in the

particle size distribution and soil texture ranged from clay to sandy loam. In all samples, the negative charges of the surface were mainly neutralised by calcium, whose average amount varied from 40.8 to 13.1 $cmol_c\ kg^{-1}$. The amount of pedogenic iron oxides was instead more homogenous (around 17 $g\ kg^{-1}$), with the exception of the cambic horizon from Mollisols where the DCB-extractable Fe was more than 30 $g\ kg^{-1}$.

The total pore volume of the aggregates (V_{HgT}, Table 3) varied from minimum values of 94-102 $mm^3\ g^{-1}$ in cambic and C horizons of Mollisols, respectively, to a maximum of 162 $mm^3\ g^{-1}$ in ochric epipedons of Inceptisols. The analysis of the cumulative curve of the intruded Hg volume allowed to identify, in all samples, a bimodal distribution of pores. The average size of *Rf* varied between 0.010 and 0.024 µm with small variations among soil orders or horizons. The lowest mean V_{Hgf} was found in the cambic horizons of Inceptisols (28 $mm^3\ g^{-1}$). The V_{Hgf} was correlated to the volume of clay (*Vsf*, r=0.697, p<0.001, n=29), without any deviation of specific soil orders or horizons from the general trend (Figure 1A-B). However, only one half of the variance of V_{Hgf} was explained by the volume of finer particles (r^2=0.486). The average size of *Rc* showed a high variability, particularly in Mollisols where it ranged from 0.292 to 2.776 µm (Table 3). Larger *Rc* did not give rise to higher pore volumes, and in fact V_{Hgc} increased from C to A horizons in all soil orders, ranging from 31 to 131 $mm^3\ g^{-1}$ independently from *Rc* size. Also for the coarser fraction a significant correlation between the volume of pores and solids was found (r=0.687, p<0.001; n=29), and the amount of variance explained by the corresponding solid particle volume was even lower than for V_{Hgf}. The maximum and minimum values of total porosity measured by Hg porosimetry were obviously found in the horizons with the highest and lowest V_{HgT} and corresponded on the average to 0.29 and 0.21 (Table 4).

The total ideal porosity (Φ_{ideal}) was calculated for each sample. In agreement with Koltermann and Gorelick (1995, see Figures 2a-2f page 3286), the minimum computed Φ_{ideal}

occurred around 0.2-0.3 of clay mass fraction (Figure 2), corresponding to the theoretical complete filling of voids among larger particles (Clarke, 1979).

The ideal model systematically underpredicted porosities (Table 4). The disagreement between the experimental and the predicted porosities was reported as Φ_{HgT}/Φ_{ideal} ratio in Figure 3. As visible, the experimental data were up to five times higher than the porosities predicted with the ideal model. The least developed soil order had the lowest mean underprediction, which was significantly lower than that of Inceptisols (Figure 3A). Among horizons, the largest underprediction was found in the most developed horizons (i.e. cambic and mollic horizons together), where the Φ_{HgT}/Φ_{ideal} ratio was significantly higher than in the other samples (Figure 3B).

The organic carbon was linked to the Φ_{Hg}/Φ_{ideal} ratio, but the linear relationship was strongly dependent on the type of soil horizon and on the contents of organic matter (Figure 4). In the subsurface horizons, independently from the diagnostic characteristics, the low amount of OC was significantly correlated with the Φ_{Hg}/Φ_{ideal} ratio ($r=0.580$, $p<0.01$, $n=18$; Figure 4), and even small increases in OC caused rather large increases in structural complexity. Also in the ochric and mollic epipedons the organic carbon was positively correlated with Φ_{HgT}/Φ_{ideal} ratio ($r=0.585$, $p<0.05$, $n=11$), but the variations in the OC content induced a less marked increase of the Φ_{Hg}/Φ_{ideal} ratio with respect to the results obtained for deeper horizons (Figure 4). The relation between OC/N and Φ_{HgT}/Φ_{ideal} ratios for the whole dataset is shown in Figure 5A. In this case surface and subsurface horizons had a similar relationship, but the correlation coefficient was rather low ($r=0.528$, $p<0.05$, $n=29$). Nonetheless, when the data were split into surface/subsurface horizons, the correlation between OC/N and Φ_{Hg}/Φ_{ideal} ratio increased and, in surface horizons, it was independent from soil orders ($r=0.713$, $p<0.01$, $n=11$, Figure 5B). In deeper horizons, the OC/N ratio was positively correlated only in the case of Inceptisols and Mollisols ($r=0.859$, $p<0.01$, $n=11$, Figure 5C) and no significant correlation was found for

Entisols. The percentage of variance explained by these relations was 51% for all surface horizons and 74%, for the subsurface horizons of Inceptisols and Mollisols.

4. Discussion

A bimodal pore size distribution was detected by mercury porosimetry in aggregates of all soil orders and all soil horizons, in agreement with the typical characteristics of natural porous media (Bruand and Prost, 1987; Vidal Vázquez et al., 2008). In the near surface horizons, the main portion of the pore volume corresponded to large pore radii (~ 0.3-2.8 μm), while smaller pores (0.01-0.02 μm) contributed more to the total pore volume in deeper soil horizons . The presence of the largest pore radius has been previously described both on artificial sand-clay mixtures and natural soil aggregates, and related to the packing of coarser particles (Fiès, 1992; Balbino et al., 2002). Smaller pores originate instead from the intrusion of Hg in the clay-fabric pore space (Fiès, 1992). In our samples, both V_{Hgc} and V_{Hgf} were related to particle size distribution, thereby confirming that porosity was influenced by simple packing structures, as in unstructured sediments and ideal porosity models. The regressions however indicated that more than 50% of the variability of the pore space remained unexplained and should therefore be related to additional factors.

Several easily measurable soil properties are known to influence porosity in a broad sense, but are not sufficient to characterise the pore system of a specific soil (e.g. Pachepsky et al., 2006). Some Authors identified morphological characteristics as basic indicators to predict soil physical properties, but the approach was mainly non-quantitative, i.e. nominal variables (e.g. Calhoun et al., 2001).

In our samples, the quantitative underestimate of aggregate porosity (the Φ_{HgT}/Φ_{ideal} ratio) was related to degree of soil development, and thus the lack of fit observed in the Φ_{ideal} model was most likely the result of pedological structural organisation. Even if the soils developed on

different parent materials, no effects of this variable could be detected. The influence of parent material on soil properties decreases with soil development (Schaetzl and Anderson, 2005), but no differences in Φ_{HgT}/Φ_{ideal} ratio were found to be caused by the presence of different substrata, not even in the C horizons (p=0.403, n=9, oneway-anova). The highest mean values of the Φ_{HgT}/Φ_{ideal} ratio were found in Eutrusteps and in their cambic horizons or in the mollic epipedons of Haplustolls, thus at the most advanced stages of development for the soil orders and horizons we have studied.

Soil structure development is controlled by different mechanisms and agents in different soil types (Bronick and Lal, 2005), but the main factor that modify aggregation and thus acts on the soil porous system in a wide range of soils is organic matter (OM). Its relevance however depends on its quantity and quality (Abiven et al., 2009). With increasing contents of organic matter, the Φ_{Hg}/Φ_{ideal} ratio increased, suggesting the interference of organic compounds on the simple sterical arrangement of soil particles. The effect is however much less pronounced in surface horizons than in deeper ones, where OM is only one of the factors that affect soil structure. In surface horizons of poorly developed soils, a high content of organic matter is mainly linked to the accumulation of poorly selected labile compounds that promote a rapid formation of aggregates by means of transient binding agents (Kay, 1998). By taking into account the data reported by Stanchi et al. (2008), whose set of samples partially overlaps with ours, we computed the increase in particle density after oxidation with H_2O_2 ($\rho_{sH2O2} - \rho_s$) in four ochric (two from Entisols and two from Inceptisols) and one mollic epipedons with OC contents from 26.8 to 62.4 g kg^{-1}. The H_2O_2 treatment preserves the oldest and stable organic matter (von Lützow et al., 2007) and, consequently, $\rho_{sH2O2} - \rho_s$ should provide an estimate of the amount of easy oxidisable, labile OM. In these five samples, the $\rho_{sH2O2} - \rho_s$ varied from 0.05 to 0.71 g cm^{-3} and was strongly positively related with the Φ_{HgT}/Φ_{ideal} ratio ($r=0.965$, $p<0.01$), thus there is a first evidence of the effect of the labile organic matter pool

on aggregate structure development. Also the OC/N ratio, which is a common indicator of the whole OM pool turnover (Bronick and Lal, 2005), was related to the porosity underestimate by the ideal packing model, and indicated that the complexity of soil aggregate structure increased with the reduction of the degree of transformation (higher OC/N ratio) of organic compounds. Both indicators pointed therefore to a marked effect of less transformed and less chemically selected organic compounds in the building up of aggregate structural organisation in surface horizons. This result stresses the mutual relationship between OM and soil aggregate structure (Blanco-Canqui and Lal, 2004) as the encapsulation within soil aggregates offers a physical protection against microbial attack to the most labile compounds (Baldock and Skjenstad, 2000). However, the relation between the quality of OM and the Φ_{Hg}/Φ_{ideal} was valid for all three soil orders, but explained only 50% of the variability of the underprediction. It was evident therefore that neither the quantitative, nor the qualitative data could fully explain the effects OM had on structural development. This may be due to a soil-specific role of the organic matter. It has long been recognised (Oades and Waters, 1991) that when the OM transformation process has proceeded enough, as in mollic epipedons, more stable organic compounds can form hierarchically organised aggregates. This aggregation type is less expressed in other surface horizons of well-developed soil orders, such as Alfisols or Oxisols (Six et al., 2004). The formation of microaggregates, or of microaggregate-within-macroaggregates, originates smaller pores (Dexter, 1988), and this mechanism may account for the smaller *Rc* values we obtained in the samples from mollic epipedons. This more complex organisation of aggregates, with persistent behaviour, could be superimposed on the former transient process, resulting in an actual porosity that deviates more from the ideal in mollic epipedons than in the other A horizons.

The OM quantity and quality affected the pore system also in the subsurface horizons, but in a different way with respect to the topsoils and with some differences also among soil orders. In

the subsurface horizons, an increase in OM induced a more marked increase in the Φ_{Hg}/Φ_{ideal} ratio than in the A horizons. In addition, the structural complexity was strongly related to the OC/N ratio in Inceptisols and Mollisols, while no significant relation was found in Entisols. In deeper horizons, OM accumulation is coupled with other pedogenic processes, such as the weathering of the mineral phases. Weathering induces a change of the rock structure, through the alteration of soil primary minerals and the release of elements that may in turn generate soil clay minerals and oxides (Hudnall et al., 2000). The presence of secondary minerals introduces a new factor into structure development, because the interactions among particles will strongly depend on their charge and not only on their size, as in ideal packing or in structureless sediments. Thus, the more marked effect of OM on structural complexity we found in deep horizons is likely to be only apparent and linked to the concomitant presence of secondary minerals and inorganic binding agents. Here, aggregation and the consequent spatial particle arrangement can also be affected by oxides and by polyvalent cations (Six et al., 2004). Due to the neutral to basic soil pH, close to the point of zero charge of the most common iron (hydr)oxides, the effect of oxides in these soils should be minimal, and indeed we did not find any relation between the Φ_{Hg}/Φ_{ideal} ratio and the DCB-extractable Fe (Table 2). The pH-dependent surface charges of iron oxides should in fact be neutralised or slightly negatively charged, thus preventing electrostatic interactions with the negatively charged clay particles or organic compounds. Among polyvalent cations, only Ca is likely to play a role in aggregation, again because of the soil pH: we found a significant positive correlation between the Φ_{Hg}/Φ_{ideal} ratio and the amount of exchangeable calcium, but only in subsurface horizons of Inceptisols ($r=0.839$, $p=0.018$, $n=7$). This relation indicates that, where the weathering process has acted on the formation of secondary clay minerals, calcium is a co-dominant factor in structural development through the formation of clay-polyvalent cation-organic matter complexes. In the deeper horizons of the least developed soils, pedogenic processes

had a minimal effect on soil properties, the porosity underestimate was relatively low, and not even specifically related to the OM quality or inorganic binding agents. The paucity of pedogenic transformation products may explain the low degree of aggregate structural complexity and induces a porous system which still retains some of the characteristics of the sediments.

5. Conclusions

Soil Taxonomy is primarily a morphological taxonomic system, but with strong genetic underpinnings (Schaetzl and Anderson, 2005). In our soil samples, the evolutionary degree defined on the basis of the taxonomic characteristics was well related to physical properties of aggregates. In fact, depending on soil orders and horizons, samples exhibited different and complex porous systems. The porosities predicted thought the ideal model based on textural data were up to fivefold underestimated and the highest disagreement between predicted and measured porosities was found where pedogenesis has been more intense, allowing to relate aggregate structure organisation to different pedogenic processes.

The OC contributed to the development of structure though OM accumulation both as labile compounds and whole OM, but a simplified linear approach could not adequately explain its soil-specific effect, in turn controlled by the predominant process.

The relation between organic carbon and Φ_{HgT}/Φ_{ideal} ratio stresses the well-known relation between OM and aggregate: OM is a factor responsible for structure development, but aggregates exert an effect on OM dynamics though the retention of less decomposed fractions. This relation operates in all surface horizons, but the effect OM has on structural complexity is maximised only when other pedogenic processes have proceeded enough.

References

Abiven, S., Menasseri, S., Chenu, C., 2009. The effects of organic inputs over time on soil aggregate stability – A literature analysis. Soil Biol. Biochem. 41, 1-12.

Balbino, L.C., Bruand, A., Brossard, M., Grimaldi, M., Hajnos, M., Guimarães, F., 2002. Changes in porosity and microaggregation in clayey Ferralsols of Brazilian Cerrado on clearing for pasture. Eur. J. Soil Sci. 53, 219–230.

Baldock, J.A., Skjemstad, J.O., 2000. Role of the soil matrix in protecting natural materials against biological attack. Org. Geochem. 31, 697-710.

Blanco-Canqui, H., Lal, R. 2004. Mechanisms of carbon sequestration in soil aggregates. Crit. Rev. Plant Sci. 23, 481-504.

Bockheim, J.G., Gennadiyev, A.N. 2000. The role of soil-forming processes in the definition of taxa in Soil Taxonomy and the World Soil Reference Base. Geoderma 95, 53-72.

Bremner, J.M., Mulvaney, C.S., 1982. Nitrogen – Total, in: Page, A.L., Miller, R.H., Keeney, D.R. (Eds.), Methods of soil analysis, part 2, 2nd edition. American Society of Agronomy, Madison, Wisconsin, pp. 595-624.

Bronick, C.J., Lal, R., 2005. Soil structure and management: a review. Geoderma 12, 3-32.

Bruand, A., Prost, R., 1987. Effect of water content on the fabric of soil material: an experimental approach. J. Soil Sci. 38, 461–472.

Calhoun, F.G., Smeck, N.E., Slater, B.L., Bigham, J.M., Hallet, G.F., 2001. Predicting bulk density of Ohio Soils from Morphology, Genetic Principles, and Laboratory Characterization Data. Soil Sci. Soc. Am. J. 65, 811-819.

Clarke, R.H., 1979. Reservoir properties of conglomerates and conglomeratic sandstones. AAPG Bulletin 63, 799-809.

Costantini, E.A.C., Urbano,F., L'Abate,G., 2004. Soil regions of Italy. http://www.soilmaps.it

Dexter, A.R., 1988. Advances in characterization of soil structure. Soil Till. Res. 11, 199-238.

Edwards, A.P., Bremner, J.M., 1967. Microaggregates in soils. J. Soil Sci. 18, 64-73.

Falsone, G., Bonifacio, E., 2009. Pore-size distribution and particle arrangement in fragipan and nonfragipan horizons. J. Plant Nutr. Soil Sci. 172, 696-703.

Fiès, J.C., 1992. Analysis of soil textural porosity relative to skeleton particle size, using mercury porosimetry. Soil Sci. Soc. Am. J. 56, 1062–1067.

Fiès, J.C., Bruand, A., 1998. Particle packing and organization of the textural porosity in clay-silt-sand mixtures. Eur. J. Soil Sci. 49, 557–567.

Gee, G.W., Bauder, J.W., 1986. Particle-size analysis, in: Klute, A. (Ed.), Methods of soil analysis Part 1: Physical and mineralogical methods. SSSA, Madison, pp. 383-411.

Hudnall, W.H., West, L.M., Benham, E.C., Wilding, L.P., 2000. Inceptisols, in: Sumner, M.E (Ed.), Handbook of soil science. CRC Press, Boca Raton, pp. E-242-255.

Kamann, P.J., Ritzi, R.W., Dominic, D.F., Conrad, C.M., 2007. Porosity and permeability in sediment mixtures. Ground Water 45, 429-438.

Kay, B.D., 1998. Soil structure and organic carbon: a review, in: Lal, R., Kimble, J.M., Follet, R.F., Stewart, B.A. (Eds.), Soil processes and the carbon cycle. CRC Press, Boca Raton, pp. 169-197.

Koltermann, C.E., Gorelick, S.M., 1995. Fractional packing model for hydraulic conductivity derived from sediment mixtures. Water Resour. Res. 31, 3283-3297.

Lowell, S., Shields, J.E., 1991. Powder surface area and porosity. Chapman and Hall, London, UK, pp. 90-98.

Mehra, O.P., Jackson. M.L., 1960. Iron oxide removal from soils and clays by a dithionite-citrate system buffered with sodium bicarbonate. Clays and Clay Minerals. Proc. 7th National Conf. on Clays and Clay Minerals, Washington, DC, 1958, 317-327.

Nelson, D.W., Sommers, L.E., 1982. Total carbon, organic carbon and organic matter, in: Page, A.L., Miller, R.H., Keeney, D.R. (Eds.), Methods of soil snalysis, part 2, 2nd edition. American Society of Agronomy, Madison, Wisconsin, pp. 539-579.

Newhall, F., 1972. Calculation of soil moisture regimes from the climatic record, Revision 4. USDA Soil Conservation Service, Washington DC.

Nordt, L.C., Collins, M.E., Fanning, D.S., Monger, H.C., 2000. Entisols, in: Sumner, M.E. (Ed.), Handbook of soil science. CRC Press, Boca Raton, pp. E-224-241.

Oades, J.M., Waters, A.G., 1991. Aggregate hierarchy in soils. Aust. J. Soil Res. 29, 815-828.

Pachepsky, Y.A., Rawls, W.J., Lin, H.S., 2006. Hydropedology and pedotransfer functions. Geoderma 131, 308-316.

Rhoades, J.D. 1982. Cation Exchange Capacity, in: Page, A.L., Miller, R.H., Keeney, D.R. (Eds.), Methods of soil analysis, part 2, 2nd edition. American Society of Agronomy, Madison, Wisconsin, pp. 149-157.

Rühlmann, J., Körschens, M., Graefe, J., 2006. A new approach to calculate the particle density of soils considering properties of the soil organic matter and the mineral matrix. Geoderma 130,272-283.

Schaetzl, R.J., Anderson, S., 2005. Soils: genesis and geomorphology. Cambridge University Press, NY, USA.

Six, J., Bossuyt, H., Degryze, S., Denef, K., 2004. A history of research on the link between (micro)aggregates, soil biota, and soil organic matter dynamics. Soil Till. Res. 79, 7-31.

Skopp, J.M., 2000. Physical properties of primary particles, in: Sumner, M.E. (Ed.), Handbook of soil science. CRC Press, Boca Raton, pp. A-3-17.

Soil Survey Staff , 1999. Soil Taxonomy, a basic system of soil classification for making and interpreting soil surveys. 2nd edn., Agriculture Handbook No. 436, US Department of Agriculture, Natural Resources Conservation Service, Washington, DC, USA.

Stanchi, S., Bonifacio, E., Zanini, E., Perfect, E. 2008. Chemical and physical treatment effects on aggregate breakup in the 0-to 2 mm size range. Soil Sci. Soc. Am. J. 72, 1418-1421.

Tisdall, J.M., Oades, J.M., 1982. Organic matter and water-stable aggregates in soils. J. Soil Sci. 62, 141-163.

Van Wambeke, A.R., 2000. The Newhall Simulation Model for estimating soil moisture and temperature regimes. Cornell University, Ithaca, NY USA.

Vidal Vázquez, E., Paz Ferreiro, J., Miranda, J.G.V., Paz González, A., 2008. Multifractal analysis of pore size distributions as affected by simulated rainfall. Vadose Zone J. 7, 500-511.

von Lützow, M., Kögel-Knabner, I., Ekschmitt, K., Flessa, H., Guggenberger, G., Matzner, E., Marschner, B., 2007. SOM fractionation methods: relevance to functional pools and to stabilization mechanisms. Soil Biol. Biochem. 39, 2183-2207.

Washburn, E.W., 1921. Note on a method of determining the distribution of pore sizes in a porous material. Proceedings of the National Academy of Sciences 7, 115–116.

Zanini, E., E. Bonifacio, N. Alliani, and V. Boero. 1995. Genesi e caratteri chimici, mineralogici e strutturali dei suoli marginali dell'Appennino Lucano. Miner. Petrogr. Acta. 38:177–188.

Table 1. General information on soils

Elevation (m a.s.l.)	Aspect (°N)	Slope (%)	Parent material	USDA classification	Studied genetic horizons	Munsell Color of horizons (moist) *Munsell Color of horizons (dry)*	Structure of horizons [§] grade-size-type
456	20	20	marls	Typic Haplustoll	A, C	7.5YR3/2, 7.5YR6/1 *7.5YR4/4, 7.5YR7/2*	2-f-gr, 3-m-abk
580	23	40	carbonates	Typic Ustorthent	AC, C	2.5YR4/3, 5YR5/3 *2.5YR5/4, 5YR6/3*	1-f-gr, 1-f-abk
670	32	42	sandstones	Typic Eutrustept	A, Bw1, Bw2, C	10YR3/1, 10YR4/3, 2.5YR4/3, 10YR4/6 *10YR3/2, 10YR4/4, 2.5YR4/4, 10YR5/6*	1-f-gr, 1-f-abk, 3-m-abk, 1-m-abk
680	315	15	marls	Typic Haplustoll	A, C	10YR3/2, 10YR4/3 *10YR4/3, 10YR5/3*	2-m-gr, 2-m-abk
800	32	40	conglomerates	Typic Ustorthent	A, AC, C	2.5YR3/3, 2.5YR3/4, 5YR4/6 *2.5YR3/4, 2.5YR4/4, 5YR5/6*	1-f-gr, 1-f-gr, 2-f-abk
870	23	45	argillites	Typic Ustorthent	A, AC, C	10YR3/3, 10YR3/4, 10YR4/3 *10YR4/4, 10YR4/4, 10YR5/3*	2-f-gr, 2-f-abk, 1-f-abk
1015	135	50	conglomerates	Typic Ustorthent	A, AC	7.5YR3/3, 7.5YR3/4 *7.5YR3/4, 7.5YR4/4*	1-f-gr, 1-f-abk
1100	0	30	marls	Typic Haplustoll	A, Bw, C	5YR3/2, 2.5YR3/3, 10R3/3 *5YR3/3, 2.5YR3/4, 10R3/4*	2-f-gr, 3-m-gr, 0
1200	10	20	marls	Typic Eutrustept	A, Bw, C1, C2	10YR3/3, 10YR4/3, 10YR4/4, 10YR3/4 *10YR3/4, 10YR5/3, 10YR5/4, 10YR4/4*	2-f-abk, 3-f-abk, 3-m-abk, 0
1200	13	25	argillites	Lithic Ustorthent	A1, A2	5YR3/2, 7.5YR3/4 *5YR3/3, 7.5YR4/4*	1-f-gr, 1-f-gr
1200	135	10	argillites	Typic Eutrustept	A, C	10YR3/2, 10YR4/4 *10YR3/3, 10YR5/6*	2-fr-gr, 2-co-abk

[§] Codes according Schoenenberger et al. (2002). Grade: 0 structureless, 1 weak, 2 moderate, 3 strong; Size: f fine, m medium, co coarse; Type: gr granular, abk angular blocky

Table 2. Selected physicochemical properties of the soil samples

Orders	Genetic horizons	Diagnostic horizons	n		pH	OC ($g\ kg^{-1}$)	OC/N	sand (%)	silt (%)	clay (%)	CEC ($cmol_c\ kg^{-1}$)	Ca_{exch} ($cmol_c\ kg^{-1}$)	Fe_{DCB} ($g\ kg^{-1}$)
Entisols	A	ochric	5	mean	7.3	22.9	8.5	55.7	25.9	18.4	29.2	20.3	18.3
				st. dev.	*0.8*	*9.8*	*0.7*	*19.3*	*8.1*	*17.8*	*7.8*	*4.3*	*5.3*
	AC	-	4	mean	8.0	8.9	9.8	54.1	17.7	28.3	21.6	19.1	17.6
				st. dev.	*0.6*	*4.2*	*3.6*	*21.8*	*9.7*	*19.6*	*6.8*	*5.4*	*12.4*
	C	-	3	mean	7.6	3.9	7.4	51.0	16.9	32.0	21.8	17.0	14.3
				st. dev.	*1.3*	*2.2*	*1.1*	*26.5*	*9.6*	*22.2*	*8.9*	*6.6*	*9.0*
Inceptisols	A	ochric	3	mean	7.0	47.5	12.5	60.2	23.0	16.8	27.8	22.5	19.8
				st. dev.	*1.2*	*22.7*	*2.9*	*8.4*	*4.8*	*10.2*	*5.8*	*7.0*	*11.3*
	Bw	cambic	3	mean	8.0	11.5	9.9	46.1	27.4	26.5	18.1	15.7	15.2
				st. dev.	*0.9*	*4.7*	*1.2*	*6.4*	*7.3*	*1.2*	*2.3*	*3.0*	*0.7*
	C	-	4	mean	7.2	5.0	6.7	44.0	30.5	25.6	17.2	13.1	19.1
				st. dev.	*1.0*	*1.8*	*0.9*	*12.4*	*8.6*	*5.5*	*1.4*	*1.6*	*11.5*
Mollisols	A	mollic	3	mean	7.7	36.0	10.7	42.9	35.1	22.0	29.4	23.9	16.2
				st. dev.	*0.3*	*9.4*	*2.7*	*9.8*	*5.0*	*5.2*	*7.6*	*9.8*	*10.2*
	Bw	cambic	1	mean	7.8	7.1	7.1	41.9	22.7	35.4	44.1	40.8	31.6
	C	-	3	mean	8.0	4.2	5.2	41.2	29.8	28.9	29.3	26.8	13.6
				st. dev.	*0.8*	*0.2*	*1.4*	*21.8*	*13.2*	*9.9*	*9.0*	*8.7*	*4.8*

OC: organic carbon; OC/N: organic carbon to total nitrogen ratio; CEC: cation exchange capacity; Ca_{exch}: exchangeable calcium; Fe_{DCB}: sodium dithionite-citrate-bicarbonate extractable-iron

Table 3. Total volume of intruded Hg and pore characteristics obtained from the analysis of the cumulative Hg-intrusion curves

Orders	Genetic horizons	Diagnostic horizons	n		V_{HgT} ($mm^3\ g^{-1}$)	*Rf* (µm)	*Rc* (µm)	V_{Hgf} ($mm^3\ g^{-1}$)	V_{Hgc} ($mm^3\ g^{-1}$)	*Vsf* ($mm^3\ g^{-1}$)	*Vsc* ($mm^3\ g^{-1}$)	*Vf* ($mm^3\ g^{-1}$)	*Vc* ($mm^3\ g^{-1}$)
Entisols	A	ochric	5	mean	149	0.012	1.302	42	107	73	323	115	431
				st. dev.	*57*	*0.012*	*0.792*	*36*	*72*	*70*	*73*	*102*	*137*
	AC	-	4	mean	113	0.013	1.050	42	71	110	280	152	351
				st. dev.	*31*	*0.013*	*0.764*	*44*	*28*	*76*	*77*	*114*	*105*
	C	-	3	mean	118	0.012	1.060	61	56	125	264	186	320
				st. dev.	*15*	*0.013*	*0.878*	*33*	*23*	*87*	*86*	*118*	*109*
Inceptisols	A	ochric	3	mean	162	0.017	0.557	31	131	69	337	100	469
				st. dev.	*16*	*0.011*	*0.611*	*8*	*8*	*43*	*37*	*47*	*32*
	Bw	cambic	3	mean	119	0.010	1.106	28	91	104	288	132	379
				st. dev.	*10*	*0.004*	*0.920*	*8*	*15*	*4*	*6*	*10*	*20*
	C	-	4	mean	112	0.016	1.112	43	69	99	290	143	358
				st. dev.	*26*	*0.006*	*0.992*	*16*	*36*	*21*	*22*	*34*	*57*
Mollisols	A	mollic	3	mean	152	0.009	0.292	36	116	88	313	125	428
				st. dev.	*19*	*0.001*	*0.151*	*18*	*36*	*21*	*18*	*4*	*18*
	Bw	cambic	1	mean	94	0.010	2.776	46	48	138	252	184	300
	C	-	3	mean	102	0.024	1.345	71	31	112	276	184	307
				st. dev.	*19*	*0.011*	*0.713*	*18*	*1*	*39*	*39*	*54*	*38*

V_{HgT}: total volume of intruded Hg; *Rf* and *Rc*: modal pore radius of finer and coarser fractions; V_{Hgf} and V_{Hgc}: volume of voids of finer and coarser fractions; *Vsf* and *Vsc*: volume of solids of finer and coarser fractions; *Vf* and *Vc*: total volume of finer and coarser fractions

Table 4. Porosity measured by Hg porosimetry (Φ_{HgT}) and porosity predicted with the ideal packing model (Φ_{ideal}). Data are dimensionless.

Orders	Genetic horizons	Diagnostic horizons	n		Φ_{HgT}	Φ_{ideal}
Entisols	A	ochric	5	mean	0.27	0.20
				st. dev.	*0.07*	*0.08*
	AC	-	4	mean	0.22	0.13
				st. dev.	*0.05*	*0.05*
	C	-	3	mean	0.23	0.15
				st. dev.	*0.01*	*0.04*
Inceptisols	A	ochric	3	mean	0.29	0.13
				st. dev.	*0.01*	*0.06*
	Bw	cambic	3	mean	0.24	0.07
				st. dev.	*0.03*	*0.02*
	C	-	4	mean	0.22	0.10
				st. dev.	*0.03*	*0.03*
Mollisols	A	mollic	3	mean	0.28	0.09
				st. dev.	*0.03*	*0.03*
	Bw	cambic	1	mean	0.21	0.11
	C	-	3	mean	0.21	0.15
				st. dev.	*0.04*	*0.03*

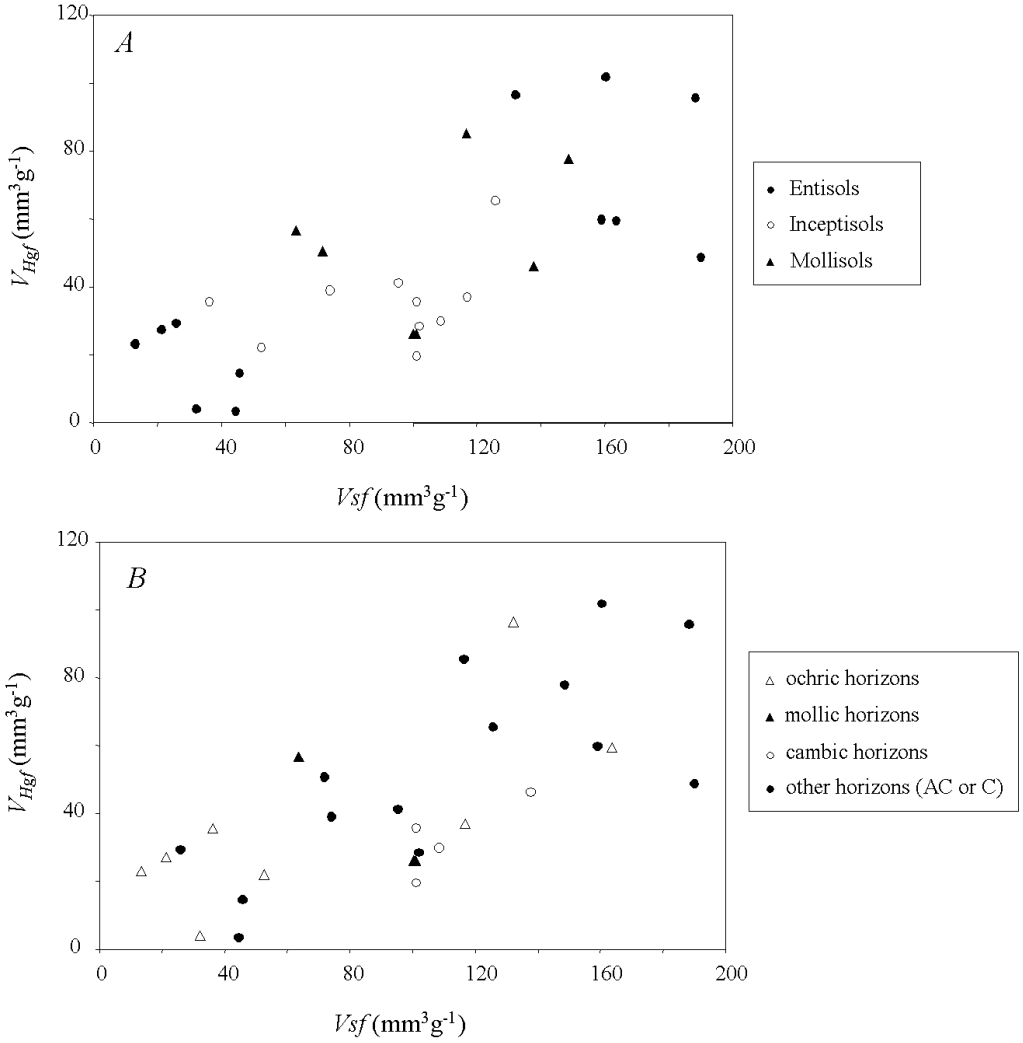

Figure 1. Relation between the total volume of solids (*Vsf*) and of pores (V_{Hgf}) of finer fraction: A) soil orders; B) soil horizons

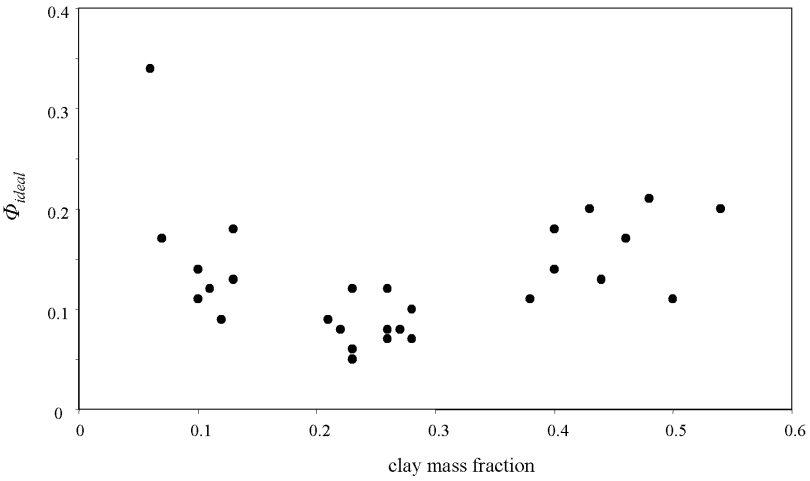

Figure 2. Clay content versus porosities predicted with ideal packing model (Φ_{ideal}).

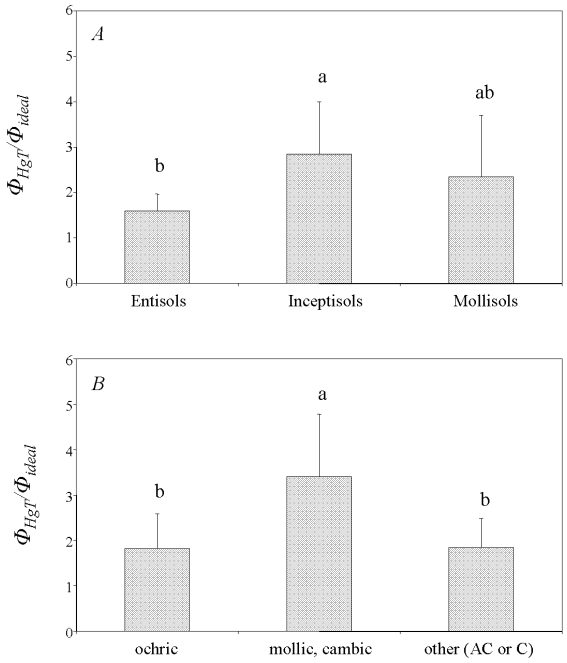

Figure 3. Mean values of porosity underestimation (Φ_{Hg}/Φ_{ideal}) obtained by the ideal packing model in: A) soil orders; B) soil horizons. Bars correspond to the standard deviation of the mean. The letters show the significant differences at p level <0.05 (Duncan's test)

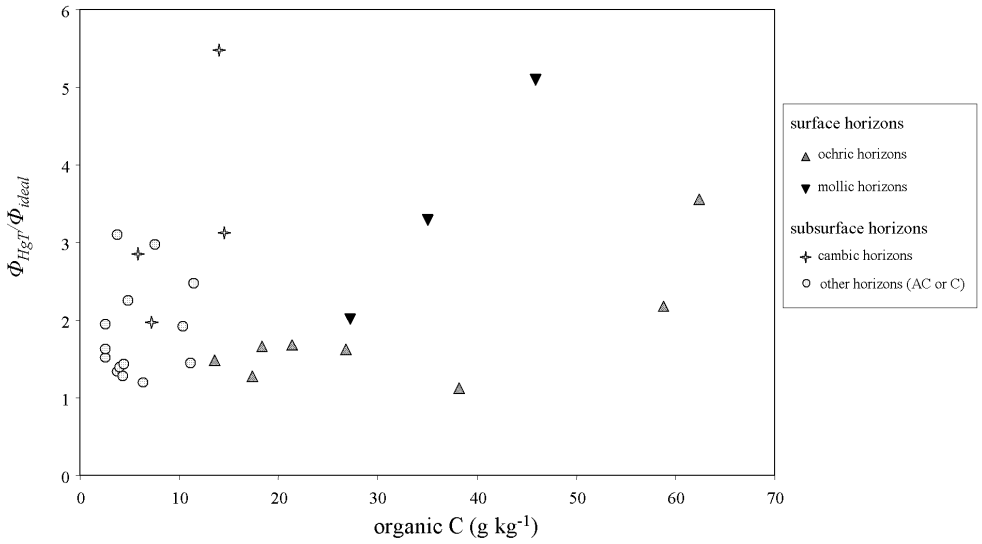

Figure 4. Organic carbon content versus porosity underestimation (Φ_{Hg}/Φ_{ideal}). Correlation coefficients are 0.585 and 0.580 (p always <0.05) for surface and subsurface horizons, respectively

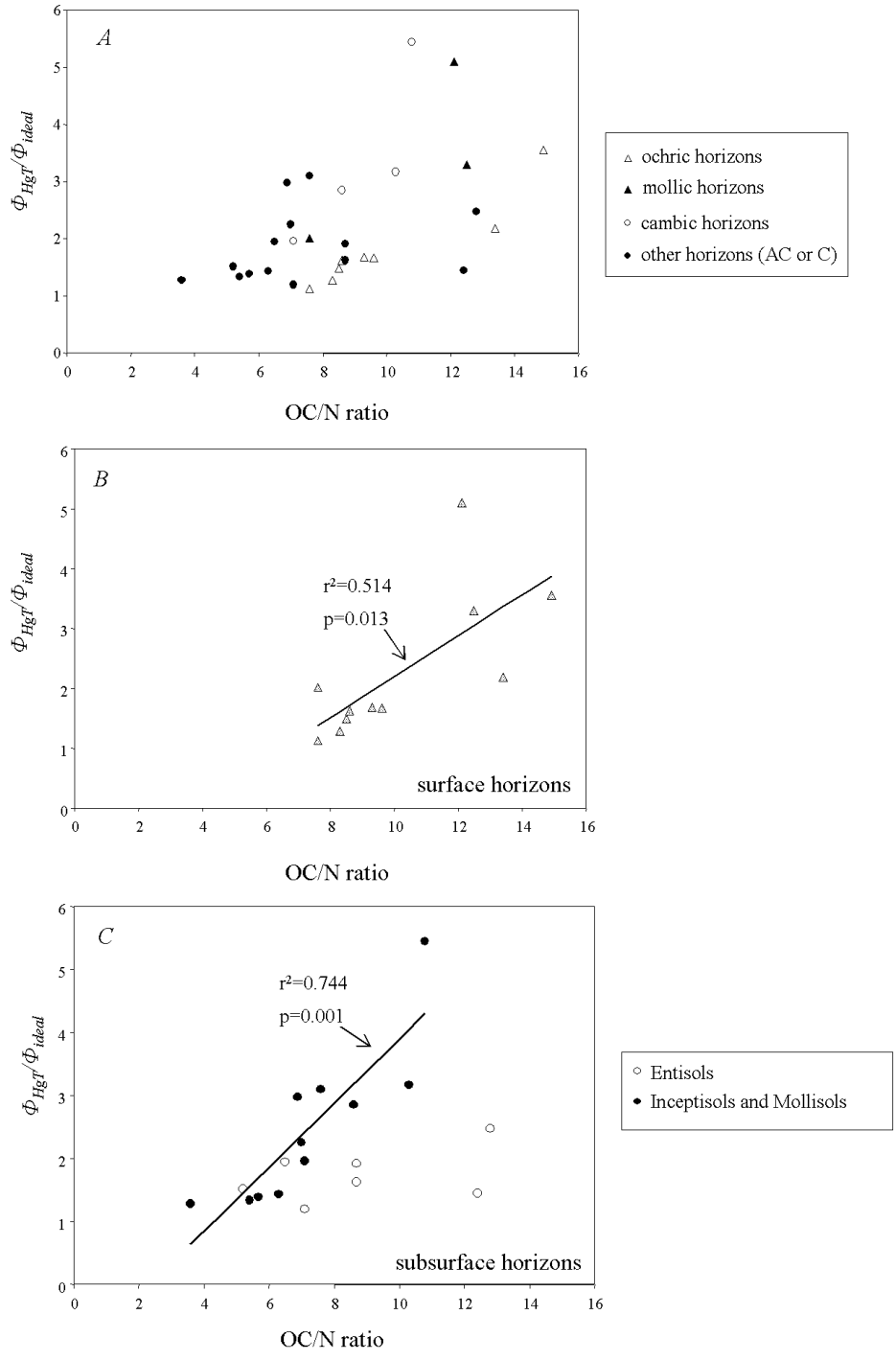

Figure 5. Organic carbon-to-total nitrogen ratio (OC/N) versus porosity underestimate (Φ_{Hg}/Φ_{ideal}): A) all samples; B) linear regression computed for surface horizons; C) linear regression computed for subsurface horizons of Inceptisols and Mollisols, the regression was not significant in subsurface horizons of Entisols